INAF
ISTITUTO NAZIONALE
DI ASTROFISICA
NATIONAL INSTITUTE
FOR ASTROPHYSICS

Publication Year	2020
Acceptance in OA	2025-02-20T11:39:34Z
Title	A Supernova Candidate at z = 0.092 in XMM-Newton Archival Data
Authors	Novara, Giovanni, ESPOSITO, PAOLO, TIENGO, ANDREA, Vianello, Giacomo, SALVATERRA, Ruben, BELFIORE MONDONI, Andrea, DE LUCA, Andrea, D'AVANZO, Paolo, Greiner, Jochen, SCODEGGIO, MARCO, Rosen, Simon, Delvaux, Corentin, PIAN, Elena, CAMPANA, Sergio, Lisini, Gianni, MEREGHETTI, Sandro, ISRAEL, Gian Luca
Publisher's version (DOI)	10.3847/1538-4357/ab98f8
Handle	http://hdl.handle.net/20.500.12386/36106
Journal	THE ASTROPHYSICAL JOURNAL
Volume	898

The Astrophysical Journal, 898:37 (8pp), 2020 July 20 https://doi.org/10.3847/1538-4357/ab98f8
© 2020. The American Astronomical Society. All rights reserved.

A Supernova Candidate at $z = 0.092$ in XMM–Newton Archival Data

Giovanni Novara[1,2], Paolo Esposito[1,2], Andrea Tiengo[1,2,3], Giacomo Vianello[4], Ruben Salvaterra[2], Andrea Belfiore[2], Andrea De Luca[2,3], Paolo D'Avanzo[5], Jochen Greiner[6], Marco Scodeggio[2], Simon Rosen[7,8], Corentin Delvaux[6], Elena Pian[9], Sergio Campana[5], Gianni Lisini[1], Sandro Mereghetti[2], and G. L. Israel[10]
[1] Scuola Universitaria Superiore IUSS Pavia, Palazzo del Broletto, piazza della Vittoria 15, I-27100 Pavia, Italy; giovanni.novara@iusspavia.it, paolo.esposito@iusspavia.it
[2] INAF–Istituto di Astrofisica Spaziale e Fisica Cosmica di Milano, via A. Corti 12, I-20133 Milano, Italy
[3] Istituto Nazionale di Fisica Nucleare (INFN), Sezione di Pavia, via A. Bassi 6, I-27100 Pavia, Italy
[4] Department of Physics, Stanford University, 382 via Pueblo Mall, Stanford, CA 94305-4013, USA
[5] INAF–Osservatorio Astronomico di Brera, via E. Bianchi 46, I-23807 Merate (LC), Italy
[6] Max-Planck-Institut für extraterrestrische Physik (MPE), Giessenbachstrasse 1, D-85740 Garching, Germany
[7] European Space Astronomy Center (ESA/ESAC), Operations Department, Vilanueva de la Cañada, E-28692 Madrid, Spain
[8] Department of Physics and Astronomy, University of Leicester, LE1 7RH Leicester, UK
[9] INAF–Osservatorio di Astrofisica e Scienza dello Spazio, via P. Gobetti 101, I-40129 Bologna, Italy
[10] INAF–Osservatorio Astronomico di Roma, via Frascati 33, I-00078 Monteporzio Catone, Italy
Received 2020 February 21; revised 2020 May 29; accepted 2020 June 1; published 2020 July 21

Abstract

During a search for X-ray transients in the XMM–Newton archive within the EXTraS project, we discovered a new X-ray source that is detected only during an ∼5 min interval of an ∼21 hr-long observation performed on 2011 June 21 (EXMM 023135.0–603743, probability of a random Poissonian fluctuation: $\sim 1.4 \times 10^{-27}$). With dedicated follow-up observations, we found that its position is consistent with a star-forming galaxy (SFR = 1–2 $M_{\odot}$ yr^{-1}) at redshift $z = 0.092 \pm 0.003$ ($d = 435 \pm 15$ Mpc). At this redshift, the energy released during the transient event was 2.8×10^{46} erg in the 0.3–10 keV energy band (in the source rest frame). The luminosity of the transient, together with its spectral and timing properties, make EXMM 023135.0–603743 a gripping analog to the X-ray transient associated to SN 2008D, which was discovered during a Swift/XRT observation of the nearby ($d = 27$ Mpc) supernova-rich galaxy NGC 2770. We interpret the XMM–Newton event as a supernova shock break-out or an early cocoon, and show that our serendipitous discovery is broadly compatible with the rate of core-collapse supernovae derived from optical observations and much higher than that of tidal disruption events.

Unified Astronomy Thesaurus concepts: Core-collapse supernovae (304); X-ray bursts (1814); X-ray observatories (1819)

1. Introduction

High energy transients for the most part are discovered in the hard-X/gamma-ray band by instruments monitoring a large fraction of the sky. In the soft X-ray band ($E < 10$ keV), instead, the most sensitive instruments have small fields of view (less than a few tenths of a squared degree). However, some missions carrying narrow-field X-ray instruments have spent a long time in orbit, accumulating many years of exposure time, which makes the serendipitous discovery of rare transient events possible during observations of unrelated targets. In particular, XMM–Newton has been in orbit since 1999 December and has the largest effective area among current imaging X-ray telescopes. It is therefore the ideal mission to search for faint transients in the soft X-ray band.

One of the objectives of EXTraS,[11] a European Union −funded project aimed at mining the XMM–Newton archival data in the time domain (De Luca et al. 2016), was the identification of short-lived transient X-ray sources. In particular, we developed an algorithm to search for new point sources that were sufficiently bright only for a small fraction of the observation and could not be detected by a standard analysis of the full exposure. Such X-ray sources are therefore not included in the XMM–Newton serendipitous source catalogs released by the XMM–Newton Survey Science Centre[12] (Rosen et al. 2016).

We performed a systematic analysis of all the observations used for the 3XMM-DR5 catalog (Rosen et al. 2016) and, after the careful screening of the results, we derived a catalog of 136 new transients with a duration <5000 s, which is publicly available through the EXTraS online archive.[13] Among these transients, EXMM 023135.0–603743 is the one with the shortest duration (315 s) and is the subject of this work. In Section 2, we describe the procedures that allowed us to discover this transient. In Section 3, we report on the results of the timing and spectral analysis of the X-ray data, while Section 4 is devoted to the follow-up optical observations we carried out. The discussion of the nature of the transient follows in Section 5, together with some considerations of the rate of such events and the perspectives for future missions.

2. EXTraS Pipeline to Search for X-Ray Transients

2.1. Data Preparation

The European Photon Imaging Camera (EPIC) on board XMM–Newton consists of one pn (Strüder et al. 2001) and two MOS (Turner et al. 2001) CCD cameras sensitive to photons

[11] Exploring the X-ray Transient and variable Sky; see http://www.extras-fp7.eu.

[12] See http://xmmssc.irap.omp.eu/.

[13] See the EXTraS Transient Catalogue at http://www88.lamp.le.ac.uk/extras/query/extras_transients.

with energy between 0.2 and 12 keV. Each camera is installed behind an X-ray telescope with 58 nested grazing-incidence mirrors and focal length of 7.5 m.

The EPIC data were processed with version 14.0.0 of the Scientific Analysis Software (SAS). The analysis was performed only on events with valid pattern (0–4 for the pn and 0–12 for the MOS) and FLAG = 0 (to avoid pixels close to CCD boundaries and dead columns). In contrast to the standard analysis, the search for new X-ray sources was performed without the exclusion of the time periods in which the particle background was particularly high.

2.2. The EXTraS Procedure

The EXTraS process aimed at the discovery of new transients consists of the division of each EPIC observation into subexposures and in the search for new point sources that might have been bright only for short time intervals. In order to search over a broad range of timescales, the time-resolved source detection is applied to time intervals of variable duration, determined through a preliminary search for an excess of counts in limited time periods in small regions of the detector.

This step of the analysis is performed using the Bayesian Blocks (BB) algorithm (Scargle 1998; Scargle et al. 2013) in the 0.2–12 keV, 0.5–2 keV, and 2–10 keV energy bands. This adaptive-binning algorithm finds statistically significant changes in the count rate by maximizing the fitness function for a piecewise-constant representation of the data, starting from an event list.

To reduce the number of spurious detections and to sample a broad range of time intervals, we modified the BB algorithm to account for changes in the background rate. The new algorithm can deal with highly variable background such as that found in XMM–Newton data during soft-proton flares. For each observation, the field of view is divided in partially overlapping $30'' \times 30''$ box regions and the BB algorithm is run on each of them. Regions with no significant variability with respect to the local background light curve return only one *block* (a time bin) covering the whole observation, while regions containing candidate transients return more blocks.

To evaluate properly the background light curve and minimize the contribution from the possible variability of known sources, the BB algorithm excludes regions of source-intensity-dependent size around the point sources detected in the full observation. To also examine these regions where interesting transients might appear (especially in crowded X-ray fields, such as star-forming regions and nearby galaxies), we developed a specific algorithm. For each observation, it creates images integrated over a fixed time interval (1000 s) of regions with sides of $40''$ around the sources excluded by the BB algorithm and tests for the presence of excesses in addition to known sources on a grid of fixed positions by a sliding-cell search. After performing this analysis on each time bin, all intervals where the same source was active are merged. Among the time segments identified either in this way or by the BB analysis, we selected only those with durations shorter than 5 ks (the minimum duration of standard EPIC exposures) and coming from regions with a spatial distribution of the events that are better fit (at $>5\sigma$ confidence level) with the addition of a point source rather than by a simple isotropic background.

In the time interval obtained from the merged segments, a source detection based on the SAS task emldetect is performed on the combined EPIC MOS and pn images accumulated in the five standard 3XMM energy bands (0.2–0.5, 0.5–1, 1–2, 2–4.5, and 4.5–12 keV). The sources detected with DET_ML > 6 in the cumulative 0.2–12 keV band[14] are compared with the reference source list for the whole observation, looking for new point-like X-ray sources. We retain as good transient candidates only the new sources detected within the box that started the new corresponding Bayesian block.

After the exclusion of bright pixels and particle tracks, we obtained about 1000 transient candidates from ∼7800 3XMM-DR5 observations. The candidates with the largest likelihood of detection DET_ML (we set the threshold at DET_ML > 15, leading to 596 sources) were visually screened to exclude spurious detections or persistent sources erroneously classified as transients. The result of this screening process is the publicly available EXTraS transient catalog, which contains 136 new transient X-ray sources. Among them, EXMM 023135.0–603743 was detected in the shortest time interval (315 s; see Figure 1).

3. EXMM 023135.0–603743: XMM–Newton Data Analysis and Results

3.1. Detection Parameters and Astrometry

In the observation where EXMM 023135.0–603743 was discovered (obs. ID: 0675010401, started on 2011 June 21, exposure time of approximatively 77 ks, see Table 1), the two MOS and the pn cameras were set in Full Frame mode (time resolution of 2.6 s and 73.4 ms, respectively); all detectors were operated with the thin optical-blocking filter.

The main parameters characterizing the detection of EXMM 023135.0–603743 are reported in Table 1. To refine its position, we performed an astrometric correction by cross-matching the brightest sources detected in the XMM–Newton observation with the USNO B1 optical catalog (Monet et al. 2003). The IRAF tasks geomap and geoxytran were used to estimate the roto-translation between the X-ray and USNO B1 optical coordinates of the reference sources and calculate the corrected X-ray coordinates of EXMM 023135.0–603743: R.A. = $02^{h}31^{m}34\overset{s}{.}9$, decl. = $-60°37'43\overset{''}{.}3$ (J2000). The 1σ error radius, which was calculated as the sum in quadrature of the systematic astrometric error ($1\overset{''}{.}3$ rms) and the statistical error on the coordinates measured for the source, is $1\overset{''}{.}9$. Within this uncertainty, the position of EXMM 023135.0–603743 is consistent with a blue galaxy visible in the 2nd Digitized Sky Survey images and with no redshift reported in literature.

3.2. Light Curve and Spectrum

The EPIC background-subtracted light curve of the source and the background (extracted from circles with radii of 20 and 60 arcsec, respectively) in the 0.5–5 keV energy band (the band in which the signal-to-noise ratio is maximized) are shown in Figure 2. Although the background is very strong and variable, a significant count-rate excess is visible ∼28 ks after the start of the observation. As shown in Figure 2, this flare can be fit with a Gaussian centered at 2011 June 21 18:50:54 ± 30 s UT and with $\sigma = (146 \pm 22)$ s. Integrating the Gaussian, we derive that the flare is formed by 47 cts in the 0.5–5 keV band. The

[14] This is the standard detection threshold adopted for the XMM–Newton source catalogs; DET_ML = $-\ln(p)$, where p is the probability that the count excess was due to a random Poissonian fluctuation (see Cash 1979, and http://xmm-tools.cosmos.esa.int/external/sas/current/doc/emldetect/node3.html for an extensive description of the parameter).

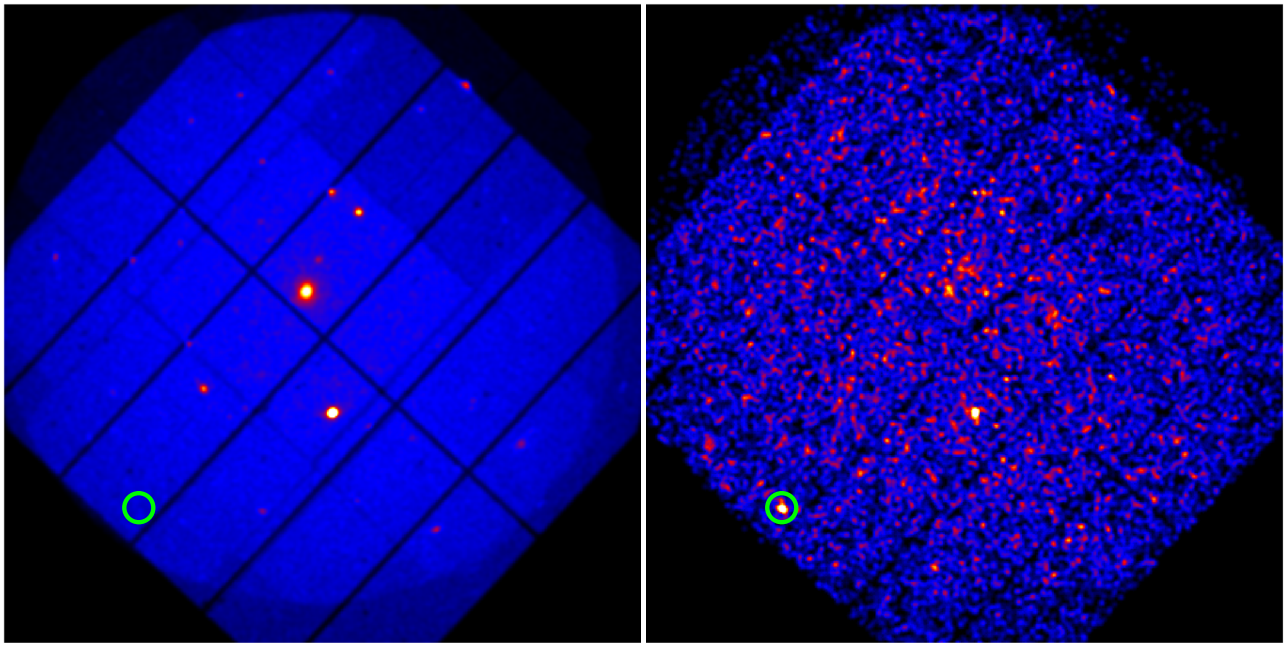

Figure 1. EPIC images (0.2–12 keV, combined pn and MOS data) with Gaussian smoothing accumulated from the full exposure (left panel) and only during the 315 s time interval in which the transient was detected (right panel). The green circles (40″ radius) indicate the position of the X-ray transient.

Table 1
Parameters of EXMM 023135.0–603743 in Observation 0675010401

Parameter	EPIC	pn	MOS1	MOS2
DET_ML[a]	61.8	30.3	13.8	20.1
SCTS[a]	54.7	27.3	11.1	16.3
Exposure time (ks)	⋯	60.2	75.8	76.9

Notes. The detection likelihood is indicated by DET_ML (see note 4), while SCTS is the number of net counts.
[a] In the 0.2–12 keV energy range and only in the 315 s time interval in which EXMM 023135.0–603743 was detected.

addition of a constant component to the model is not required, with a 3σ upper limit of 7.4×10^{-4} cts s^{-1}, which means that the emission outside the flare is perfectly consistent with the background level. More complicate, asymmetric models are not required to describe the flare (see also the discussion in Section 5.1).

The X-ray spectrum of the transient was extracted from a circle with 40 arcsec radius in the 315 s interval during which it was detected and the corresponding background spectrum from a nearby source-free region. The spectral analysis was carried out with the fitting package XSPEC and adopting the abundances by Wilms et al. (2000). Using a power-law model absorbed both in our Galaxy (we fixed the column value in the XSPEC model component tbabs to $N_{\rm H,Gal} = 3 \times 10^{20}$ cm^{-2}; Dickey & Lockman 1990; Kalberla et al. 2005) and in the host galaxy (ztbabs with $z = 0.092$, see Section 4.1), we derive a photon index $\Gamma = 2.6^{+0.7}_{-0.6}$ and a >95% evidence for higher-than-Galactic absorption, indicating a local component in the host galaxy, $N_{\rm H,z} = (1.0^{+0.6}_{-0.5}) \times 10^{22}$ cm^{-2}. The goodness of the fit, evaluated as the percentage of Monte Carlo realizations that had Cash statistics (C-stat) lower than the best-fitting C-stat, is 86% (we performed 10^4 simulations). The average luminosity (for $d = 435$ Mpc, see Section 4.1) was $\approx 9 \times 10^{43}$ erg s^{-1} in the 0.3–10 keV band (in the source rest frame). Therefore, the total energy of the flare was 2.8×10^{46} erg. The peak luminosity was 1.2×10^{44} erg s^{-1} and the 3σ upper limit on the persistent X-ray luminosity outside the flare interval is 2.8×10^{41} erg s^{-1}. A somewhat better fit (76% of the realizations with C-stat lower than the best-fit one) is obtained with a blackbody model. The temperature is equivalent to $0.57^{+0.10}_{-0.08}$ keV and for the local absorption we obtain $N_{\rm H,z} = 1.5 \times 10^{21}$ cm^{-2}, but the value is loosely constrained and consistent with zero. Assuming this model, the total energy emitted was 8×10^{45} erg.

4. Follow-up Optical Observations of EXMM 023135.0–603743

4.1. CTIO/Blanco Telescope Observations

We observed the field of EXMM 023135.0–603743 with the 4 m CTIO/Blanco telescope equipped with the COSMOS spectrograph. A series of three consecutive spectra, each one lasting 900 s, was obtained on 2016 July 12 starting at 09:20 UT. The spectroscopic observations were executed using a 1.3 arcsec slit, the r2K grism (GG455 filter), covering the 4955–9023 Å wavelength range with a dispersion of 1 Å pixel^{-1}. The spectral reduction and extraction were carried out using standard procedures under the ESO-MIDAS[15] package. The wavelength calibration has been checked against sky emission lines. From the detection of several emission (Hβ, [O III], Hα, [N II]) and absorption lines, we derived a redshift $z = 0.092 \pm 0.002$ (Figure 3). With the cosmological parameters in Planck Collaboration et al. (2016, assumed throughout the paper), this redshift corresponds to a luminosity distance $d = 435 \pm 15$ Mpc (Wright 2006).

4.2. La Silla (MPG/ESO 2.2 m GROND)

The transient field was observed with the seven-channel imager GROND (Greiner et al. 2008) on 2016 July 30 starting

[15] See http://www.eso.org/projects/esomidas/.

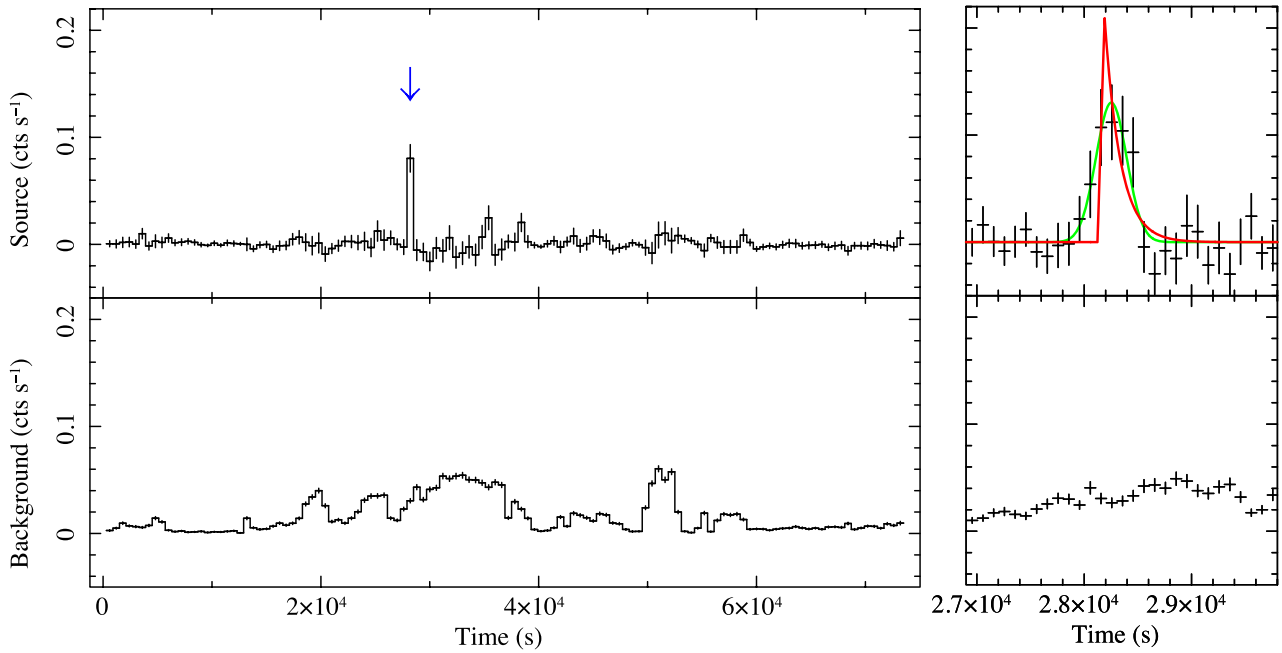

Figure 2. Left panel, top: EPIC background-subtracted light curve extracted from a 20 arcsec radius circle in the 0.5–5 keV energy band with 10 minute time bins. The blue arrow indicates the flare of EXMM 023135.0–603743. Left panel, bottom: corresponding background light curve extracted from a nearby circular region with 60 arcsec radius and rescaled to the area of the source extraction region. Right panel: same as on the left, but with 100 s time bins and closing up on the source. The lines show the fits with a Gaussian (green) and a FRED (red) model (see Section 5.1 for details); in the latter, the burst rise time and e-folding decay time are fixed to the best-fit values derived for SN 2008D in Soderberg et al. (2008).

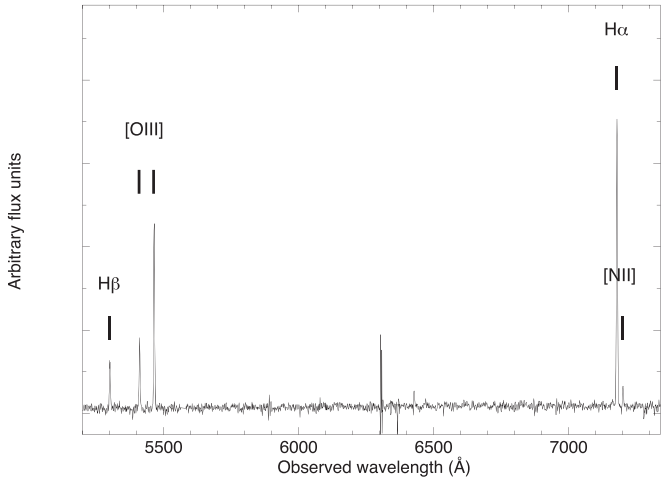

Figure 3. CTIO/Blanco telescope optical spectrum of the host galaxy of EXMM023135.0603743 at $z = 0.092 \pm 0.002$.

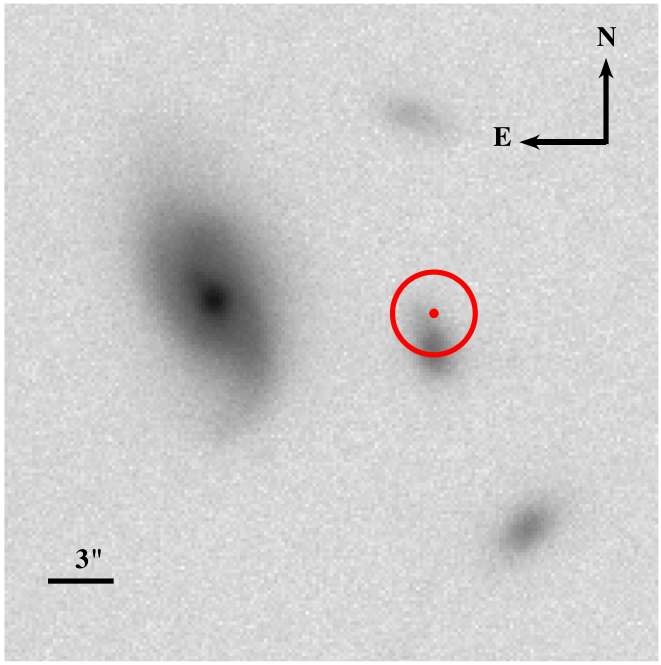

Figure 4. GROND optical image (30″ side). The red circle indicates the position of the X-ray transient and its 1σ uncertainty (1.9″ radius) derived after astrometric correction against the USNO catalog (the position of five common X-ray and optical sources have been used to register the image). Note that also the astrometry of the GROND image was performed using the USNO catalog. The only object for which we could find an entry in a catalog is the galaxy east (at ∼12″) of the transient, PGC361816 in the HyperLEDA database (Makarov et al. 2014).

at 08:30 UT at ∼1″ seeing (Figure 4). The effective exposure was 36 minutes in $g'r'i'z'$, and 30 minutes in *JHK*. The GROND data were reduced in the standard manner (Krühler et al. 2008) using pyraf/IRAF (Tody 1993; Yoldaş et al. 2008). The optical/NIR imaging was calibrated against the Gaia SkyMapper Southern Sky Survey[16] (Gaia Collaboration et al. 2018; Wolf et al. 2018a) catalogs for $g'r'i'z'$, and the 2MASS catalog (Skrutskie et al. 2006) for the *JHK* bands. This results in typical absolute accuracies of ±0.03 mag in $g'r'i'z'$ and ±0.05 mag in *JHK*.

From the available optical and near-infrared photometry (Table 2), and the optical spectrum, it is possible to derive some basic physical properties of the host galaxy. We have used the GOSSIP spectral energy distribution (SED) fitting package (Franzetti et al. 2008) to model the SED of the galaxy, starting from the multiband photometric information, and using the PEGASE2 population synthesis models

[16] See http://skymapper.anu.edu.au.

Table 2
GROND Photometry

Photometric Band	Magnitude
g'	19.58 ± 0.01
r'	19.58 ± 0.01
i'	19.53 ± 0.01
z'	19.67 ± 0.02
J	19.39 ± 0.07
H	19.63 ± 0.14
K	19.67 ± 0.18

Note. All magnitudes are in the AB system and are corrected for the foreground Galactic extinction.

(Fioc & Rocca-Volmerange 1997) coupled with a family of delayed star formation histories (Gavazzi et al. 2002) to derive the spectral templates. From the properties of the best-fitting SED model, we estimate a galaxy stellar mass of $\approx$(2–3) $\times$ 10^8 $M_\odot$, an absolute B-band magnitude of -18.49, and a star formation rate SFR $\approx$ 1 $M_\odot$ yr^{-1}. For and independent check, we also used the Le PHARE (Arnouts et al. 1999; Ilbert et al. 2006) package with 70 templates from both the PEGASE2 and BC03 (Bruzual & Charlot 2003) and we found that predictions of the best-fitting individual templates fall within the ranges (1.5–3) $\times$ 10^8 $M_\odot$ for the mass and 0.1–1 $M_\odot$ yr^{-1} for the SFR.

A direct measurement of the galaxy SFR can also be obtained from the Hα line luminosity, as measured from the galaxy optical spectrum. To have a reliable absolute flux calibration for the spectrum, we scaled the spectroscopic fluxes so that the magnitude one can derive by integrating the spectroscopic flux over the r-band photometric passband matches the r-band magnitude from the GROND photometry. After this rescaling, the observed flux of the Hα line, as derived by fitting a combination of a Gaussian profile for the emission line and a second-order polynomial for the underlying background, is of 9.8×10^{-15} erg cm^{-2} s^{-1}, corresponding to a luminosity of 2.2×10^{41} erg s^{-1}. From this luminosity, following the recipe by Kennicutt (1998), we can derive an estimate of the current star formation rate of SFR $= 1.7\, M_\odot$ yr^{-1}.

5. Discussion

5.1. An X-Ray Flare Associated to a Supernova

The energy released in the flare, its duration and spectrum, as well as the properties of the host galaxy, recall the characteristics of the X-ray transient associated to SN 2008D in NGC 2770, which was observed with Neil Gehrels Swift Observatory's XRT and interpreted as the X-ray emission from the shock break-out of a core-collapse supernova (Soderberg et al. 2008, see also Modjaz et al. 2009). To explore further this analogy, we fit to the light curve of the transient a fast-rise-and-exponential-decay (FRED) model with the rise time ($t_r = 72$ s) and e-folding decay time ($t_d = 129$ s) fixed to the values reported in Soderberg et al. (2008), obtaining a marginally acceptable fit (see Figure 2). Even though the shape of the light curve is not necessarily a fingerprint of the event, to test the compatibility of the time evolution of these two supernova shock break-out candidates, we applied the two sample Kolmogorov–Smirnov (KS) test to the arrival times of their X-ray events, for a time interval of 600 s starting from the beginning of the flares. Selecting the EPIC events in the energy band 0.5–5 keV, from a 20″ circular region and applying the same selections to Swift/XRT observation (00031081002) of SN 2008D, we obtain a probability of 35% that the arrival times of the events collected during the transient EXMM 023135.0–603743 and the X-ray flare associated to SN 2008D are drawn from the same distribution. We also note that the luminosity of the X-ray emission detected in the decaying part of the Swift/XRT light curve of SN 2008D (Soderberg et al. 2008) is well below the 3σ upper limit we set on the persistent X-ray emission of EXMM 023135.0–603743. This means that, if present, a tail similar to that of SN 2008D would have escaped detection in the XMM–Newton data.

Since we discovered the X-ray transient several years after the event, we had no chance to perform follow-up optical observations to search for possible supernova light. No simultaneous optical data from the Optical Monitor (OM) on board XMM–Newton are available, since the position of the transient was outside its field of view, which is smaller than that of the EPIC cameras. However, we found archival optical data for the host galaxy from a monitoring with the Catalina Real-time Transient Survey (more specifically, the Siding Spring Survey; Drake et al. 2009), including observations performed about two months after the burst. These data are consistent with a steady source, but they are not sensitive enough to exclude the presence of a supernova, since a supernova as bright as SN 2008D (Soderberg et al. 2008) at $z = 0.092$ would have peaked at $V \approx$ 20–21 mag, which could have been detected only in much deeper exposures.

We searched for possible counterparts in other surveys of SNe and transients in the southern sky. Unfortunately, several major SN surveys started a few months or years after our event (for example, La Silla-QUEST, Baltay et al. 2013; DES,[17]; SkyMapper Southern Sky Survey, Wolf et al. 2018b; ESO VST SUDARE[18]). We also checked that the field of EXMM 023135.0–603743 was not covered by the OGLE[19] project (Udalski et al. 2015). The Transient Name Server[20] (TNS) reports four transients in a 2° neighborhood of EXMM 023135.0–603743, all of which occurred at least 5 years after our event. Among the optical SNe in a time window compatible with EXMM 023135.0–603743, the closest in sky distance is SN 2011eb (found in NGC 782, at R.A. $= 01^h57^m36\overset{s}{.}6$, decl. $= -57°48'00\overset{''}{.}8$ (J2000); Parrent et al. 2011), which is, however, more than 5° away from the XMM–Newton event, and therefore incompatible.

5.2. Other Interpretations

The similarities with the X-ray transient associated to SN 2008D suggest that also in the case of EXMM 023135.0–603743 the X-ray emission from the shock break-out of a core-collapse supernova was detected, but we examined other possible interpretations of the event. Considering that in the full EXTraS analysis we discovered only a few transients with a duration in the 100–500 s range, the possibility of chance alignment of a Galactic transient (e.g., an optically faint flaring star) with a star-forming galaxy at $z \sim 0.1$ seems remote. Following Bloom et al. (2002), we estimate that the probability to find by chance a galaxy as bright as the proposed host or brighter within 2″ from the EXTraS transient is 2.5×10^{-3}. Moreover, the evidence for an absorption in excess to the total Galactic N_H in that direction derived from the

[17] See the Dark Energy Survey at http://darkenergysurvey.org.
[18] See the ESO Messenger article at http://www.eso.org/sci/publications/messenger/archive/no.151-mar13/messenger-no151-29-32.pdf.
[19] See http://ogle.astrouw.edu.pl/.
[20] See the Transient Name Server at https://wis-tns.weizmann.ac.il.

spectral analysis (in particular, for the power-law model) is an additional indication that the X-ray transient is located outside our Galaxy.

Although the X-ray transient position coincides with a peripheral region of the galaxy (possibly the arm of a tidally disturbed spiral galaxy), it is consistent at 1σ with the center of the galaxy. However, we can rule out the possibility of a flare from an active galactic nucleus (AGN) since there is no evidence for AGN activity either in optical or at X-rays ($L_X < 2.8 \times 10^{41}$ erg s^{-1}). A 5 minute flare from a quiescent supermassive black hole cannot be excluded, but it would be an unprecedented phenomenon, since the maximum energy released in this kind of X-ray flare by Sagittarius A* is several orders of magnitude smaller (e.g., Ponti et al. 2017).

The luminosity of the event is consistent with a tidal disruption event (TDE; e.g., Burrows et al. 2011; Komossa 2015). However, the fast rise of the emission would require a rather exotic scenario: a white dwarf tidally disrupted by an intermediate-mass black hole ($<10^5$ $M_\odot$; Equation (23) of Stone & Metzger 2016, see also Jonker et al. 2013; Glennie et al. 2015; Bauer et al. 2017). Another possibility is that the flare is associated with a shock break-out of a star in the course of a "standard" tidal disruption event, before the onset of the accretion (e.g., Guillochon et al. 2009). However, both possibilities are disfavored against a supernova shock break-out by the rate of tidal disruption events, which is much lower than that of core-collapse supernovae (see Figure 6).

Another X-ray bright event with a timescale of ∼5 minutes is the pulsating tail of a giant flare from a magnetar (e.g., Kaspi & Beloborodov 2017; Esposito et al. 2018). However, we do not detect any bright initial spike and the tail energy is typically $\sim 10^{44}$ erg, about two orders of magnitude smaller than that emitted by EXMM 023135.0–603743.

5.3. Event Rate

To determine the event rate of X-ray flares as the one detected in EXMM 023135.0–603743, we have to evaluate the sensitivity of our search to this kind of event at different distances. Many instrumental effects and observation properties can strongly affect the sensitivity of our search: the intensity of the time-variable particle background, chip gaps and defects, instrument settings (operating mode and filter), the presence of bright and extended sources, Galactic interstellar absorption, and the transient spectrum, light curve, and off-axis angle. We therefore decided to evaluate the detection efficiency of our search algorithm by simulating the X-ray flare at different flux levels and detector positions and, after the addition of the simulated events to real EPIC data, applying the EXTraS pipeline to see how many of them are recovered as a function of the distance.

Since the count statistics of the X-ray flare of EXMM 023135.0–603743 is rather poor, but the transient seems to us to be analogous of the SN 2008D X-ray flare, which is much better characterized (Soderberg et al. 2008), we adopted the spectrum and the light-curve shape of the latter as a template for simulating the flares. In the spectral model of each simulated X-ray flare, we assumed the Galactic absorption expected at its sky coordinates from the survey by Kalberla et al. (2005). The positions of the simulated transients were randomly distributed in a square region with an area of 0.324 square degrees, containing the full EPIC field of view. All the relevant instrumental properties (including the point-spread function, as well as vignetting, filter transmission, and detector efficiency effects) were taken into account.

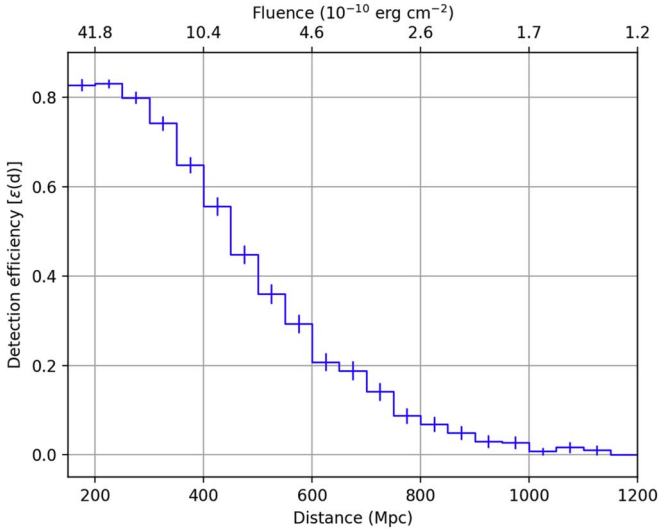

Figure 5. Detection efficiency as a function of the simulated source distances. The upper x-axis shows the corresponding 0.3–10 keV fluence of the simulated sources.

We simulated ∼100,000 transients with 0.3–10 keV fluence ranging from 10^{-10} to 5×10^{-9} erg cm^{-2} and added the simulated photons to the pn and MOS data of ∼2900 randomly selected XMM–Newton observations, corresponding to ∼40% of the 3XMM-DR5 observations. We then used the EXTraS transient pipeline (Section 2.2) to detect the simulated flares, adopting the same detection threshold (DET_ML > 15).

After filtering out the events simulated outside the field of view and in time intervals during which the instruments were not operating, 48,166 simulated sources had at least 1 valid count. We detected significantly 71% of them. In Figure 5, we show the success rate ($\epsilon(d)$) as a function of the luminosity distance, derived from the fluence of the simulated sources assuming a flare energy of 2×10^{46} erg (Soderberg et al. 2008).

This detection efficiency $\epsilon(d)$ can be used to compute the effective volume ($V_{\rm eff}$) covered by our survey as:

$$V_{\rm eff} = \sum \epsilon(d_i) V(d_i) = (4.1 \pm 0.1) \times 10^8 \,{\rm Mpc}^3, \qquad (1)$$

where $V(d_i)$ is the comoving volume in the redshift interval corresponding to the d_i distance bin in Figure 5.

The survey coverage of the EXTraS search for transients can be derived from the sum of the exposure maps[21] of all the observations included in the search. The total survey coverage is 1.1 deg^2 yr, corresponding to a coverage of the full sky for $T = 2.7 \times 10^{-5}$ yr $\simeq$ 14 minutes.

The event rate for $n = 1$ detection is therefore:

$$\frac{n}{T \times V_{\rm eff}} = (0.9^{+2.1}_{-0.7}) \times 10^{-4} \,{\rm yr}^{-1}\,{\rm Mpc}^{-3}, \qquad (2)$$

where the 1σ statistical uncertainty was computed according to Gehrels (1986). This rate is consistent (albeit within large uncertainties) with the core-collapse supernova rate by Cappellaro et al. (2015) in the $z < 0.2$ range sampled by our survey (see Figure 6).

[21] The exposure maps were not corrected for the vignetting effect and in the case of simultaneous observations by more EPIC cameras, the one with the largest value was selected.

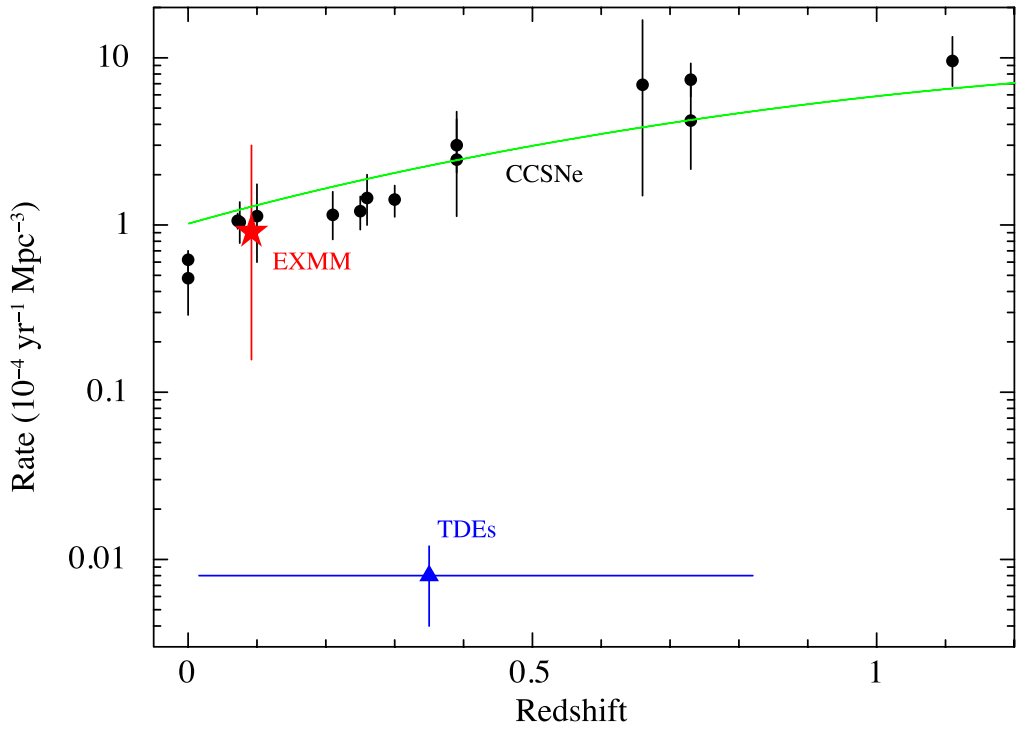

Figure 6. The core-collapse supernova data (black dots) are from Cappellaro et al. (2015, and the references therein). The green solid line shows the predicted core-collapse supernova rate from Madau & Dickinson (2014) for a Salpeter initial mass function with the lower and upper mass limits for the progenitors of 8 and 40 $M_{\odot}$. The blue triangle represents the rate of tidal disruption event (from van Velzen 2018).

It is worth noting that the host galaxy of EXMM 023135.0–603743 has a small mass and a high specific star formation rate, as expected for the majority of galaxies hosting core-collapse supernovae (Botticella et al. 2017). Also the distance of ∼400 Mpc is consistent with expectations, as a combination of volume increase and detection efficiency decrease (Figure 5) at larger distances. Soderberg et al. (2008) observed that the X-ray detection of SN 2008D was compatible with the possibility that core-collapse supernovae emit this kind of X-ray flare. Subsequent observations and studies (e.g., Mazzali et al. 2008; Modjaz et al. 2009) associate the X-ray flare of SN 2008D to an early cocoon from a massive helium star. In any case, regardless of the exact nature of the transient X-ray emission, the serendipitous discovery of EXMM 023135.0–603743 in a field galaxy rather than in the target of an observation, as in the case of SN 2008D in the supernova-rich galaxy NGC 2770, allows us to derive a more straightforward and unbiased estimate of the rate of such events.

Transients like EXMM 023135.0–603743 will become detectable up to significantly larger distances with the Athena X-ray Observatory (Barret et al. 2019). Thanks to its ∼10 times larger effective area with respect to XMM–Newton, we expect that Athena will push the 50% detection efficiency for this kind of event from $z \sim 0.1$ to $z \sim 0.28$, increasing by a factor ∼20 the accessible volume. In particular, the Wide Field Instrument (WFI) will have a field of view ∼2.5 times larger than EPIC and, therefore, Athena will be able to detect similar X-ray flares ∼50 times more frequently than XMM–Newton, which corresponds to more than 2 events per year considering equal observing time shares between the WFI and the X-IFU instruments.

A large number of events in the local universe could be detected by soft X-ray detectors with very large fields of view. For example, the THESEUS mission (Amati et al. 2018) should be able to detect ∼4 supernova shock break-outs per year within 50 Mpc in its 1 sr field of view. The accumulation of a significant number of events at different distances will soon allow us to measure the supernova rate in the X-ray band and its evolution with redshift up to $z \sim 0.3$ with a precision comparable to present measurements in optical and infrared, and with the advantage of a much smaller bias against supernovae in dusty environments.

This research has made use of data produced by the EXTraS project, funded by the European Union's Seventh Framework Programme under grant agreement No. 607452. The scientific results reported in this article are based on observations obtained with XMM–Newton, an ESA science mission with instruments and contributions directly funded by ESA Member States and NASA. This work also used observations at Cerro Tololo Inter-American Observatory (CTIO), National Optical Astronomy Observatory, which is operated by the Association of Universities for Research in Astronomy (AURA) under a cooperative agreement with the National Science Foundation. We thank Steven Heathcote for granting us CTIO director's discretionary time and the CTIO staff for performing the observations. Part of the funding for GROND (both hardware as well as personnel) was generously granted from the Leibniz-Prize to Prof. G. Hasinger (DFG grant HA 1850/28-1). This work is partly based on tools produced by GAZPAR operated by CeSAM-LAM and IAP. G.N., P.E., A.T., R.S., A.D.L., P.D. A., M.S., E.P., S.C., and S.M. acknowledge funding in the framework of the ASI–INAF contract No. 2017-14-H.0. We acknowledge the INAF computing centers of Osservatorio Astrofisico di Catania and Osservatorio Astronomico di Trieste for the availability of computing resources and support under the coordination of the CHIPP project. We are grateful to Franz

E. Bauer, Ofer Yaron, and Andrzej Udalski for useful information, and to Peter Jonker and Maryam Modjaz for comments on the manuscript.

Facilities: XMM–Newton (EPIC), CTIO: Blanco 4-m, MPG/ESO: 2.2-m/GROND.

Software: SAS (Gabriel et al. 2004), FTOOLS (Blackburn 1995), XSPEC (Arnaud 1996), GOSSIP (Franzetti et al. 2008), IRAF (Tody 1993) Le PHARE (Arnouts et al. 1999).

ORCID iDs

Giovanni Novara https://orcid.org/0000-0001-7304-9858
Paolo Esposito https://orcid.org/0000-0003-4849-5092
Andrea Tiengo https://orcid.org/0000-0002-6038-1090
Giacomo Vianello https://orcid.org/0000-0002-2553-0839
Ruben Salvaterra https://orcid.org/0000-0002-9393-8078
Andrea Belfiore https://orcid.org/0000-0002-2526-1309
Andrea De Luca https://orcid.org/0000-0001-6739-687X
Paolo D'Avanzo https://orcid.org/0000-0001-7164-1508
Jochen Greiner https://orcid.org/0000-0002-9875-426X
Marco Scodeggio https://orcid.org/0000-0002-2282-5850
Elena Pian https://orcid.org/0000-0001-8646-4858
Sergio Campana https://orcid.org/0000-0001-6278-1576
Sandro Mereghetti https://orcid.org/0000-0003-3259-7801
G. L. Israel https://orcid.org/0000-0001-5480-6438

References

Amati, L., O'Brien, P., Götz, D., et al. 2018, AdSpR, 62, 191
Arnaud, K. A. 1996, in ASP Conf. Ser. 101, XSPEC: The First Ten Years, ed. G. H. Jacoby & J. Barnes (San Francisco, CA: ASP), 17
Arnouts, S., Cristiani, S., Moscardini, L., et al. 1999, MNRAS, 310, 540
Baltay, C., Rabinowitz, D., Hadjiyska, E., et al. 2013, PASP, 125, 683
Barret, D., Decourchelle, A., Fabian, A., et al. 2019, AN, 341, 224
Bauer, F. E., Treister, E., Schawinski, K., et al. 2017, MNRAS, 467, 4841
Blackburn, J. K. 1995, in ASP Conf. Ser. 77, FTOOLS: A FITS Data Processing and Analysis Software Package, ed. R. A. Shaw, H. E. Payne, & J. J. E. Hayes (San Francisco, CA: ASP), 367
Bloom, J. S., Kulkarni, S. R., & Djorgovski, S. G. 2002, AJ, 123, 1111
Botticella, M. T., Cappellaro, E., Greggio, L., et al. 2017, A&A, 598, A50
Bruzual, G., & Charlot, S. 2003, MNRAS, 344, 1000
Burrows, D. N., Kennea, J. A., Ghisellini, G., et al. 2011, Natur, 476, 421
Cappellaro, E., Botticella, M. T., Pignata, G., et al. 2015, A&A, 584, A62
Cash, W. 1979, ApJ, 228, 939
De Luca, A., Salvaterra, R., Tiengo, A., et al. 2016, in Astrophysics and Space Science Proceedings: The Universe of Digital Sky Surveys, Vol. 42, Science with the EXTraS Project: Exploring the X-Ray Transient and Variable Sky, ed. N. Napolitano et al. (Cham: Springer), 291
Dickey, J. M., & Lockman, F. J. 1990, ARA&A, 28, 215
Drake, A. J., Djorgovski, S. G., Mahabal, A., et al. 2009, ApJ, 696, 870
Esposito, P., Rea, N., & Israel, G. L. 2018, in Timing Neutron Stars: Pulsations, Oscillations and Explosions, ed. T. Belloni, M. Mendez, & C. Zhang (Berlin: Springer)
Fioc, M., & Rocca-Volmerange, B. 1997, A&A, 326, 950
Franzetti, P., Scodeggio, M., Garilli, B., Fumana, M., & Paioro, L. 2008, in ASP Conf. Ser. 394, GOSSIP, a New VO Compliant Tool for SED Fitting, ed. R. W. Argyle, P. S. Bunclark, & J. R. Lewis (San Francisco, CA: ASP), 642
Gabriel, C., Denby, M., Fyfe, D. J., et al. 2004, in ASP Conf. Ser. 314, The XMM-Newton SAS—Distributed Development and Maintenance of a Large Science Analysis System: A Critical Analysis, ed. F. Ochsenbein, M. G. Allen, & D. Egret (San Francisco, CA: ASP), 759
Gaia Collaboration, Brown, A. G. A., Vallenari, A., et al. 2018, A&A, 616, A1
Gavazzi, G., Bonfanti, C., Sanvito, G., Boselli, A., & Scodeggio, M. 2002, ApJ, 576, 135
Gehrels, N. 1986, ApJ, 303, 336
Glennie, A., Jonker, P. G., Fender, R. P., Nagayama, T., & Pretorius, M. L. 2015, MNRAS, 450, 3765
Greiner, J., Bornemann, W., Clemens, C., et al. 2008, PASP, 120, 405
Guillochon, J., Ramirez-Ruiz, E., Rosswog, S., & Kasen, D. 2009, ApJ, 705, 844
Ilbert, O., Arnouts, S., McCracken, H. J., et al. 2006, A&A, 457, 841
Jonker, P. G., Glennie, A., Heida, M., et al. 2013, ApJ, 779, 14
Kalberla, P. M. W., Burton, W. B., Hartmann, D., et al. 2005, A&A, 440, 775
Kaspi, V. M., & Beloborodov, A. M. 2017, ARA&A, 55, 261
Kennicutt, R. C., Jr. 1998, ARA&A, 36, 189
Komossa, S. 2015, JHEAp, 7, 148
Krühler, T., Küpcü Yoldaş, A., Greiner, J., et al. 2008, ApJ, 685, 376
Madau, P., & Dickinson, M. 2014, ARA&A, 52, 415
Makarov, D., Prugniel, P., Terekhova, N., Courtois, H., & Vauglin, I. 2014, A&A, 570, A13
Mazzali, P. A., Valenti, S., Della Valle, M., et al. 2008, Sci, 321, 1185
Modjaz, M., Li, W., Butler, N., et al. 2009, ApJ, 702, 226
Monet, D. G., Levine, S. E., Canzian, B., et al. 2003, AJ, 125, 984
Parrent, J., Howell, D. A., Thomas, R. C., Nugent, P. E., & Sullivan, M. 2011, CBET, 2764, 3
Planck Collaboration, Ade, P. A. R., Aghanim, N., et al. 2016, A&A, 594, A13
Ponti, G., George, E., Scaringi, S., et al. 2017, MNRAS, 468, 2447
Rosen, S. R., Webb, N. A., Watson, M. G., et al. 2016, A&A, 590, A1
Scargle, J. D. 1998, ApJ, 504, 405
Scargle, J. D., Norris, J. P., Jackson, B., & Chiang, J. 2013, ApJ, 764, 167
Skrutskie, M. F., Cutri, R. M., Stiening, R., et al. 2006, AJ, 131, 1163
Soderberg, A. M., Berger, E., Page, K. L., et al. 2008, Natur, 453, 469
Stone, N. C., & Metzger, B. D. 2016, MNRAS, 455, 859
Strüder, L., Briel, U., Dennerl, K., et al. 2001, A&A, 365, L18
Tody, D. 1993, in ASP Conf. Ser. 52, IRAF in the Nineties, ed. R. J. Hanisch, R. J. V. Brissenden, & J. Barnes (San Francisco: ASP), 173
Turner, M. J. L., Abbey, A., Arnaud, M., et al. 2001, A&A, 365, L27
Udalski, A., Szymański, M. K., & Szymański, G. 2015, AcA, 65, 1
van Velzen, S. 2018, ApJ, 852, 72
Wilms, J., Allen, A., & McCray, R. 2000, ApJ, 542, 914
Wolf, C., Bian, F., Onken, C. A., et al. 2018a, PASA, 35, e024
Wolf, C., Onken, C. A., Luvaul, L. C., et al. 2018b, PASA, 35, e010
Wright, E. L. 2006, PASP, 118, 1711
Yoldaş, A. K., Krühler, T., Greiner, J., et al. 2008, in AIP Conf. Ser. 1000, First Results of GROND, ed. M. Galassi, D. Palmer, & E. Fenimore (Melville, NY: AIP), 227